Human Back Movement Analysis Using BSN

Zhi-Qiang Zhang, Julien Pansiot, Benny Lo and Guang-Zhong Yang
Department of Computing, Imperial College London, UK
Email: {z.zhang, jpansiot, benlo, gzy}@imperial.ac.uk

***Abstract*—Human back movement estimation is clinically important for assessing patients with back pain. Most current techniques are limited to simple spinal movement angles without consideration of surrounding muscle movement and backplane rotation and torsion. These three dimensional analysis is fraught with difficulties due to the complex nature of the movement and sensor placement. In this paper, a consistent method based on multiple Body Sensor Network (BSN) nodes for the measurement of 3D bending and twist of the back is proposed. In our method, five BSN nodes, each consisting of a three axis accelerometer, a gyroscope and a magnetometer, are placed at the human back. Euler angles are then defined to represent the orientation for human back segments, kinematics analysis is then derived. An unscented Kalman filter (UKF) is deployed to estimate the defined Euler angles. Detailed experimental results have shown the feasibility and effectiveness of the proposed measurement and analysis framework.**

***Index Terms*—Human Back Movement; Kinematics; Orientation; Kalman Filter;**

I. Introduction

Back pain is a serious health problem affecting eighty percent of people at some time in their life [1]. It is clinically important to increase our understanding of the relationship between back pain under different physiological loadings and movements. To this end, it is important to develop methods that can be used for back movement analysis under normal physiological activities rather than limited to specialist clinics and laboratory settings. The use of unobtrusive, wearable techniques can also facilitate rehabilitation programs, both mentored and self-regulated, for restoring motor functions [2].

Due to the complex nature of the back movement for common activities of daily living, accurate three-dimensional estimation of back movement is difficult. Thus far, most methods provide one or two-dimensional measurements of the spinal bending angles and many are intrusive and those involving optical sensors will require a direct line-of-sight of the infra-red markers [3] [4]. Invasive techniques, such as X-rays or pins embedded into the bone provide accurate spinal movement linking back movement affected by pathology. However, it is only possible to acquire limited dynamic patterns of the spinal movement due to the invasive nature of the technique. Furthermore, these techniques also lack of comprehensive measurements of back movement in three-dimensions [5].

With the rapid development of MEMS technology and miniaturized wireless sensor, pervasive human movement analysis using micro-sensors has attracted extensive interests in recent years [6]. Sensors are placed at the surface of body segment or the clothes to provide extensive movement information in three dimensions. These methods are typically combined with temporal sensor drift and integration errors for consistent movement reconstruction. For example, Foxlin et al. [7] proposed a complementary separate-bias Kalman filter, which was designed for head tracking applications. Luinge et al. [8] presented an improved limb orientation estimation method using a Kalman filter to estimate sensor drift for enhancing the estimation accuracy. Yun et al. [9] proposed an extended Kalman filter to estimate the orientation of human limb using combination of inertial sensors and magnetic sensors. They focused on the design of Kalman filter for real-time tracking of human body motion. Xsens [10] also has a similar framework. However, all the methods mentioned above are designed for general movement of human body segments, such as head and upper limb, and they are not applicable to the human back movement given the complex nature of the back movement. King et al [11] presented a system for monitoring the rotation of the lower back (sacrum and thoraco-lumbar junction) and femur in the sagittal plane using inertial sensors integrated with Body Sensor Network (BSN) nodes. Chhikara et al [12] also developed a wearable prototype based on BSN nodes to quantify pelvic to lumbar movement of the spine. Both methods are limited to rotational movement in the sagittal plane, which in effect represents only one dimensional back movement estimation.

Considering the importance, as well as difficulties, of human back movement estimation, an improved method for the measurement of 3D bending and twist of the back movement is proposed. In this paper, multiple BSN sensor nodes, each consisting of a three axis accelerometer, a gyroscope and a magnetometer are used. An example based on five BSN sensor nodes is used to illustrate the motion reconstruction framework, although the analysis technique is generic and can be easily extended to multiple sensors with known geometrical constraints. Euler angles are then defined to represent the orientation of back segments. Kinematics analysis for the Euler angle is then derived, and an unscented Kalman filter (UKF) is deployed to estimate the defined Euler angles. The experimental results have shown that the proposed method can estimate the human back movement with a good accuracy.

The rest of the paper is organized as follows. In Section II, the proposed human back movement analysis method is described, including system setup, process model, measurement model and Kalman filtering method. Experimental results are provided in Section III. Finally, conclusions and future work are given in Section IV.

Figure 1. The placement of BSN sensor nodes.

II. Analysis Framework

To facilitate our analysis, three coordinate systems are defined (capital X, Y, Z are used to represent the coordinate system):

1) Global coordinate frame $\mathcal{G}$: the reference coordinate system. In our system, we define X pointing down (the direction of gravity), Y pointing backward of the body, and Z pointing left to construct a right handed coordinate system.
2) Body coordinate frame $\mathcal{B}$: it is attached to a body segment whose rotation is to be measured. When a subject is at the neutral pose (N-pose, stand upright on a horizontal surface and keep arm straight alongside body vertically and thumbs forwards), the body coordinate system is aligned with the global coordinate system, and there is only translation between them.
3) Sensor coordinate frame $\mathcal{S}$: it corresponds to the axes of three orthogonally mounted inertial sensors and magnetometer in the sensor unit, and all the sensor measurements are expressed in this coordinate system.

To simplify our analysis, we define R_s^b as the rotation between the local body coordinate system and the corresponding sensor coordinate system.

A. System Setup

The proposed prototype system includes 5 BSN sensor nodes, and an additional sensor used as the base station. The sensors node are placed at left shoulder, right shoulder, upper spine, middle spine and low spine respectively as shown in figure 1. The sensor node platform is based on the BSN development kit [13], which consists of a TI MSP430 ultra low power processor, a Chipcon CC2420 RF module for wireless communications, and a light-weight Li-ion polymer battery. The BSN sensor node is integrated with an Analog Devices ADXL330 [14] for 3D acceleration measurement, an InvenSense ITG- 3200 digital gyroscope [15] for 3D angular velocity measurement, and a Honeywell HMC5843 [16] for 3D magnetic field measurement. The whole sensor node, measuring $20 \times 30 \times 17mm$ with a weight of only 10 grams, can provide abundant information for movement analysis, and it is an ideal platform for back movement analysis.

In our experiments, the sampling rate of the sensor node is set to be 33 Hz, and the data is wirelessly transmitted to the base station which is connected to a personnel computer for real-time processing and display. However, although there is a MAC layer for CC2420 RF module to deal with communication, packet loss can be significant. To overcome this problem, a TDMA-based sampling scheme is used.

In this scheme, time synchronization is implemented where the base station initiates the system by sending a SYNC message containing its own clock. Upon receiving this beacon message, each sensor node adjusts its clock to that of the server. Assuming the network has N sensor nodes, the time is divided into periodic cycles. Within each cycle, a sampling slot is used for all the sensor nodes to sample data while a predefined slot is assigned to each node to send the data back to the base station. Both during the sensing slot and transmission slot, all sensors will work without inference with each other.

B. Process Model

Since the basic purpose of this paper is to estimate the rotational movement of human back, orientation should therefore be explicitly included in the state vector. In this paper, we choose Euler angles to represent orientation of each segment of human back, where ϕ, θ and ψ , called roll, pitch, yaw respectively, represent positive rotations about the X, Y, and Z body axes respectively. However, the Euler angle representation is with singularity problem when $\theta = \pm 90$, but this was not found to produce any noticeable disturbances in practice [17]. The transformation from the global frame to the body frame can be defined by three successive rotations as:

$$R(\phi, \theta, \psi) = R_Z(\psi) R_Y(\theta) R_X(\phi) \tag{1}$$

where

$$R_X(\phi) = \begin{bmatrix} 1 & 0 & 0 \\ 0 & cos(\phi) & -sin(\phi) \\ 0 & sin(\phi) & cos(\phi) \end{bmatrix}, \tag{2}$$

$$R_Y(\theta) = \begin{bmatrix} cos(\theta) & 0 & sin(\theta) \\ 0 & 1 & 0 \\ -sin(\theta) & 0 & cos(\theta) \end{bmatrix} \tag{3}$$

and

$$R_Z(\psi) = \begin{bmatrix} cos(\psi) & -sin(\psi) & 0 \\ sin(\psi) & cos(\psi) & 0 \\ 0 & 0 & 1 \end{bmatrix} \tag{4}$$

Given the angular rate $\omega(t)$, the Euler angle integration kinematics can be written as:

$$\dot{\Theta}(t) = W(\Theta(t))\omega(t) \tag{5}$$

where $W(\Theta(t))$ is the Jacobian matrix that relates the absolute rotation angle to the angular rate, $\Theta(t) = \begin{bmatrix} \phi(t) \\ \theta(t) \\ \psi(t) \end{bmatrix}$ and $\omega(t) =$

$\begin{bmatrix} \omega_X(t) \\ \omega_Y(t) \\ \omega_Z(t) \end{bmatrix}$. The relationship between Euler angles and angular rate can be expressed as:

$$\begin{bmatrix} \omega_X(t) \\ \omega_Y(t) \\ \omega_Z(t) \end{bmatrix} = \begin{bmatrix} \dot{\phi}(t) \\ 0 \\ 0 \end{bmatrix} + R_X(\phi(t)) \begin{bmatrix} 0 \\ \dot{\theta}(t) \\ 0 \end{bmatrix} + R_X(\phi(t))R_Y(\theta(t) \begin{bmatrix} 0 \\ 0 \\ \dot{\psi}(t) \end{bmatrix} \tag{6}$$

and then we can get:

$$W(\Theta(t)) = \begin{bmatrix} 1 & sin(\phi(t))tan(\theta(t)) & cos(\phi(t))tan(\theta(t)) \\ 0 & cos(\phi(t)) & -sin(\phi(t)) \\ 0 & sin(\phi(t))/cos(\theta(t)) & cos(\phi(t))/cos(\theta(t)) \end{bmatrix} \tag{7}$$

For each segment, we define the following by 6×1 vector as the state:

$$x_t = \begin{bmatrix} \Theta(t) \\ \omega(t) \end{bmatrix} \tag{8}$$

With the state, the process model can be expressed as a linear combination of:

$$x_{t+1} = Fx_t + Ge_t \tag{9}$$

where

$$F = \begin{bmatrix} I_{3\times3} & W(\Theta(t))\Delta t \\ 0 & I_{3\times3} \end{bmatrix} \tag{10}$$

and

$$G = \begin{bmatrix} W(\Theta(t))\Delta t^2/2 \\ \Delta t \end{bmatrix}. \tag{11}$$

Δt is the sampling period, $I_{3\times3}$ is the identity matrix of order 3, and e_t is the angular acceleration, which is assumed to be zero mean Gaussian noise with variance Q.

C. Measurement Model

The measurement model relates the measurement value z to the value of the state vector x. The wearable sensor unit provides three types of measurement: acceleration, magnetic field and angular rate. The generalized form of the measurement equation h is

$$z_t = \begin{pmatrix} z_t^a \\ z_t^m \\ z_t^g \end{pmatrix} = h(x_t) + v_t = h(x_t) + \begin{pmatrix} v_t^a \\ v_t^m \\ v_t^g \end{pmatrix} \tag{12}$$

where v_t is assumed to be zero mean additional Gaussian white noise with covariance matrix V, z_t^a, z_t^m and z_t^g are all the acceleration, magnetic field and angular rate measurements respectively.

As the movement of human back is relatively stable, the 3-axis accelerometer mainly measure the gravity field vector with respect to global coordinate system resolved in sensor local coordinate system. Define $g = [g_x, g_y, g_z]^T$ as the vector of the gravitational field resolved in global coordinate system, and then the expected measurements of these fields are given by the transformation of g to the local sensor coordinate system, which can be represented as:

$$z_t^a = \begin{pmatrix} z_t^{a,X} \\ z_t^{a,Y} \\ z_t^{a,Z} \end{pmatrix} = R_s^b R(\phi(t), \theta(t), \psi(t))g + v_t^a \tag{13}$$

where v_t^a is the acceleration measurement noise.

With the proposed sensor configuration, the magnetometer measures the magnetic field. The expected measurements of this field are given by the transformation of the global magnetic field to the local sensor coordinate system. Similar to accelerometer's measurement, define $m = [m_x, m_y, m_z]^T$ as the vector of the magnetic field resolved in global coordinate system, and then the sensor measurement can be written as:

$$z_t^m = \begin{pmatrix} z_t^{m,X} \\ z_t^{m,Y} \\ z_t^{m,Z} \end{pmatrix} = R_s^b R(\phi(t), \theta(t), \psi(t))m + v_t^m \tag{14}$$

where v_t^m is the acceleration measurement noise.

Gyroscopes measure angular velocity in the local frame of each sensor. The angular velocity ω_t is already part of the state vector, leading to a simple model that relates the measured angular rate to the state as:

$$z_t^g = \begin{pmatrix} z_t^{g,X} \\ z_t^{g,Y} \\ z_t^{g,Z} \end{pmatrix} = R_s^b H x_t + v_t^g \tag{15}$$

where $H = \begin{bmatrix} 0 & I_{3\times3} \end{bmatrix}$ and v_t^g is the angular rate measurement noise.

D. Kalman Filtering

In general, the Kalman filter operates on a probability distribution in the state vector space, which is characterized by its first and second order statistical moments: mean and covariance. The process and measurement models predict and update this distribution. Unfortunately, the Kalman filter can only deal with linear and Gaussian problems, while the measurement equations here are nonlinear. The solution to this problem is the usage of an extension to the classical Kalman filter, namely the UKF, which can deal with nonlinearity well [18] [19].

At time $t-1$, we will get the Maximum A Posterior (MAP) estimation of the state vector x by a Gaussian distribution $N(\mu_{t-1}, \Sigma_{t-1})$. We can construct another Gaussian distribution for UKF recursion, and the mean is $x_{t-1}^\alpha = [{\mu_{t-1}}^T, 0, 0]^T$, while the covariance matrix is

$$P_{t-1}^\alpha = \begin{bmatrix} \Sigma_{t-1} & 0 & 0 \\ 0 & Q & 0 \\ 0 & 0 & V \end{bmatrix}$$

The constructed Gaussian distribution can be represented by a set of $2L+1$ sample points χ_{t-1}^i and weights W_{t-1}^i, denoted as sigma points $(\chi_{t-1}^i, W_{t-1}^i)$, where $i = 1, 2, \cdots, 2L+1$, $L = n_x + n_e + n_v$ and n_x, n_e and n_v are the dimensional

of state vector x, state noise e and measurement noise v respectively. Let $\lambda = \alpha^2(L+\kappa) - L$ and do the scaled unscented transformation, the sigma points will be

$$\begin{aligned}
\chi_{t-1}^0 &= x_{t-1}^\alpha \\
\chi_{t-1}^i &= x_{t-1}^\alpha + \left(\sqrt{(L+\lambda)P_{t-1}^a}\right)_i, \quad i = 1, 2, \cdots, L \\
\chi_{t-1}^i &= x_{t-1}^\alpha - \left(\sqrt{(L+\lambda)P_{t-1}^a}\right)_{i-L}, i = L+1, \cdots, 2L \\
W_{t-1}^{0,m} &= \lambda/(L+\lambda) \\
W_{t-1}^{0,c} &= \lambda/(L+\lambda) + (1-\alpha^2+\beta) \\
W_{t-1}^{i,m} &= W_{t-1}^{i,c} = \frac{1}{2(L+\lambda)}, \quad j = 1, \cdots, 2L
\end{aligned} \tag{16}$$

where κ, α, β are positive scaling parameters and $\left(\sqrt{(L+\lambda)P_{t-1}^a}\right)_i$ is the ith row or column of the matrix square root of $(L+\lambda)P_{t-1}^a$ and W_{t-1}^i is the weight associated with the ith point. Then the mean μ_t and covariance Σ_t of the state vector X_t propagate as follows: First the prediction step is performed as

$$\begin{aligned}
\chi_{i,t|t-1}^X &= F\chi_{i,t-1}^X + G\chi_{i,t-1}^W \\
\mu_{t|t-1} &= \sum_{i=0}^{2L} W_{t-1}^{i,m}\chi_{i,t|t-1}^X \\
\widetilde{\mu}_{i,t|t-1} &= \chi_{i,t|t-1}^X - \mu_{t|t-1} \\
\Sigma_{t|t-1} &= \sum_{j=0}^{2L} W_{t-1}^{i,c}(\widetilde{\mu}_{t|t-1}^i)(\widetilde{\mu}_{t|t-1}^i)^T \\
\gamma_{i,t|t-1} &= h(\chi_{i,t|t-1}^X) + \chi_{i,t-1}^V \\
\overline{z}_{t|t-1} &= \sum_{i=0}^{2L} W_{t-1}^{i,m}\gamma_{i,t|t-1}
\end{aligned} \tag{17}$$

where $\chi_{t-1}^i = \left[(\chi_{i,t|t-1}^X)^T, (\chi_{i,t|t-1}^W)^T, (\chi_{i,t|t-1}^V)^T\right]^T$ Then update step is as follow:

$$\begin{aligned}
\mu_t &= \mu_{t|t-1} + Gain_t \cdot (z_t - \overline{z}_{t|t-1}) \\
\Sigma_t &= \Sigma_{t|t-1} - Gain_t \cdot K_t \cdot (Gain_t)^T
\end{aligned} \tag{18}$$

where:

$$\begin{aligned}
\widetilde{z}_{i,t|t-1} &= \gamma_{i,t|t-1} - \overline{z}_{t|t-1} \\
K_t &= \sum_{i=0}^{2L} W_{t-1}^{i,c}(\widetilde{z}_{i,t|t-1})(\widetilde{z}_{i,t|t-1})^T \\
Cov_{t|t-1} &= \sum_{i=0}^{2L} W_{t-1}^{i,c}\widetilde{\mu}_{i,t|t-1}\widetilde{z}_{i,t|t-1} \\
Gain_t &= Cov_{t|t-1} \cdot (K_t)^{-1}
\end{aligned} \tag{19}$$

and in the process of numerical calculation, some symbols are defined as: $\mu_{t|t-1} \triangleq \mathbb{E}(x_t|\overline{z}_{1:t-1})$, $\mu_t \triangleq \mathbb{E}(x_t|\overline{z}_{1:t})$, $\overline{z}_{t|t-1} \triangleq \mathbb{E}(\overline{z}_t|\overline{z}_{1:t-1})$, $\Sigma_{t|t-1} \triangleq cov(x_t|\overline{z}_{1:t-1})$, $\Sigma_t \triangleq cov(x_t|\overline{z}_{1:t})$ and $K_t \triangleq cov(\overline{z}_t|\overline{z}_{1:t-1})$.

III. Experimental Results

Detailed experiments were conducted to evaluate the performance of the proposed method. We will focus the main results on analyzing Forward Bend, Back Twist and Side Bend.

A. Sensor Placement Initialization

At the beginning of each experiment, the subject was asked to hold the N-pose for at least five seconds for calibration. The main purpose of the calibration is to estimate the orientation difference between body segment coordinate $\mathcal{B}$ and the corresponding sensor coordinate $\mathcal{S}$, i.e., to estimate the value of R_s^b.

As mentioned earlier, when the subject was at the N-pose, the body segment coordinate system was aligned with the global coordinate system, only with a global translation between them. Meanwhile, the body was still; therefore, the accelerometer only measured the gravity. Denote the acceleration and magnetic field measured by the sensor unit at the lower spine as $g_s = (g_s^X, g_s^Y, g_s^Z)^T$ and $m_s = (m_s^X, m_s^Y, m_s^Z)^T$, we can estimate the yaw angle α_1 and pitch angle α_2 between the global coordinate and lower spine sensor coordinate as:

$$\alpha_1 = atan(g_s^Y/g_s^X)$$

and

$$\alpha_2 = atan\left(\frac{-g_s^Z}{g_s^X cos(\alpha_1) + g_s^Y sin(\alpha_1)}\right)$$

The gravity g and the magnetic field m at the global coordinate can be written as: $g = R_Y(\alpha_2)R_X(\alpha_1)^T g_s$ and $m = R_Y(\alpha_2)^T R_X(\alpha_1)^T m_s$.

When the subject keeps still at the N-pose, denote the acceleration and magnetic field measured by any sensor unit as $g_l = (g_l^x, g_l^y, g_l^z)^T$ and $m_l = (m_l^x, m_l^y, m_l^z)^T$, and then we can construct a measurement matrix in the sensor coordinates as:

$$M_{mea} = (g_l, m_l, g_l \times m_l),$$

and the respective matrix in the global coordinate is:

$$M_{glo} = (g, m, g \times m).$$

The orientation matrix R_d between the global coordinate and the sensor unit is

$$R_d = M_{mea} \cdot (M_{glo})^{-1}.$$

Because the body segment coordinate system is aligned with the global coordinate system, R_d is the rotation between the body segment coordinates $\mathcal{B}$ and the corresponding sensor coordinates $\mathcal{S}$.

B. Forward Bend

To demonstrate this, a subject was asked to bend his body forward several times, during which the rotational back movement is mainly about the Z axis in the global coordinate. Fig. 2 shows the angles that the subject rotates about the Z axis. As we can see from the figure: 1) although there are small differences among the yaw angles for upper spine, left shoulder and right shoulder, the three angles are almost

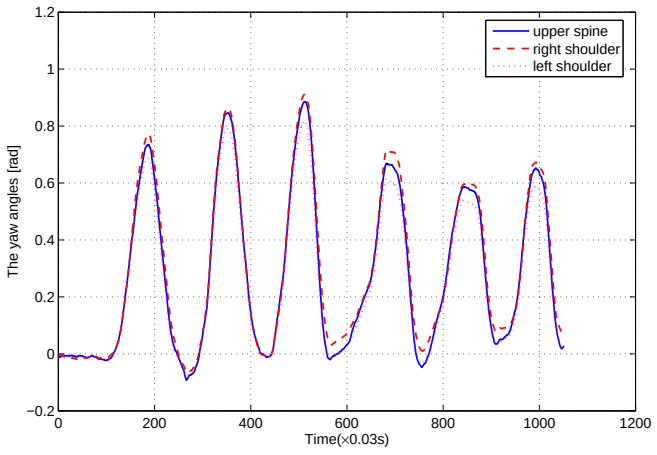

(a)

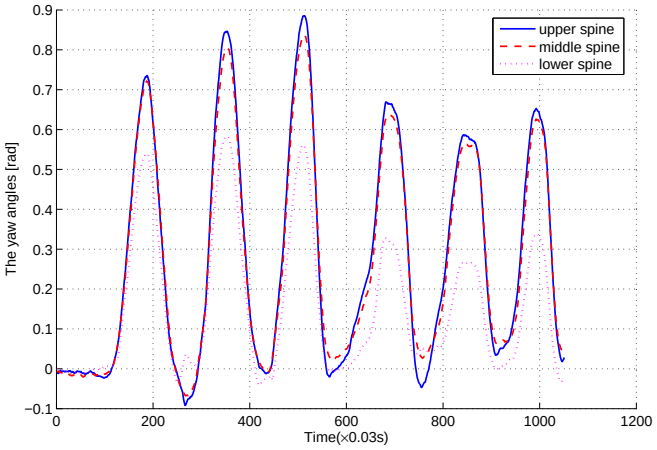

(b)

Figure 2. Yaw angles. (a) the yaw angle for upper spine, right shoulder and left shoulder; (b) the yaw angle for upper spine, middle spine and lower spine.

the same. This is mainly because the upper part of the back moves as a whole when the subject bends forward. Since in this experiment, we only used adhesive tape to stick the BSN sensor node to the subject's back, so the sensor could not always stay at the same position of the human back during the procedure of bending forward. The relative-movement between the sensor nodes and human back causes the small differences among the three estimated angles. 2) the maximum yaw angle for the upper spine at each bending is a little larger than that of the middle spine, while the maximum yaw angle for the middle spine at each bending is much larger than that of the lower spine. This is mainly because that the spine is not a rigid body, and the maximum value for different part of the spine at each bending should be different, and the maximum bending angle of the spine decreases from the top spine to the bottom spine.

It can be seen from the above results that all the roll and pitch angles for the spine and the shoulders are almost zero during the subject bends forward, which is consistent with the real situation.

C. Back Twist

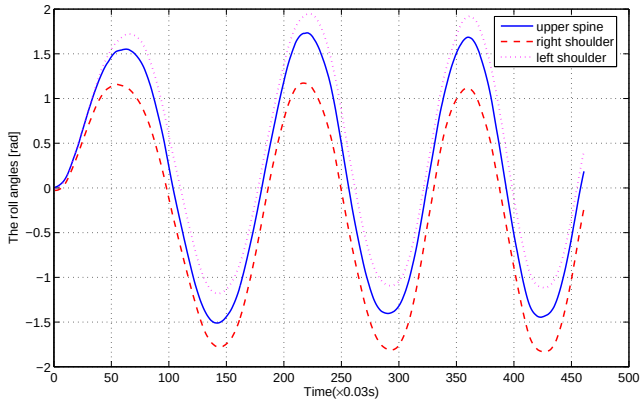

Figure 3. Roll angles for upper spine, right shoulder and left shoulder.

The subject was also asked to twist his body left and right several times, during which the rotational back movement was mainly about the X axis in the global coordinate. Fig. 3 shows the roll angles for the shoulders and the upper spine. As we can see from the figure: 1) The maximum roll angle of the left shoulder for each twisting is the largest one among the three roll angles, while the maximum roll angle for the upper spine is the second largest. This is mainly because when the subject twists right, the left upper limb pulls the left shoulder forward to keep the balance of the body, which makes the roll angle of left shoulder larger than that of the upper spine. Meanwhile, the right upper limb also pulls the right shoulder forward to keep the balance of the body, which makes the roll angle of right shoulder smaller than that of the upper spine; 2) Similar to twisting right, the roll angle of right shoulder is the largest among these three angles, and the roll angle of left shoulder is the smallest among these three angles when the subject twists his body left. As the roll angle is negative during twisting left, the roll angle of right shoulder is the smallest one in the figure.

It can also be seen that all the pitch and yaw angles for the spine and the shoulders are almost zero during the subject twists, which is consistent with the real situation. Meanwhile, the maximum twisting angle of the spine also decreases from the top spine to the bottom spine.

D. Side Bend

The subject was last asked to bend his body left and right several times, during which the rotational back movement is mainly about the Y axis in the global coordinate. Fig. 4 shows the pitch angles that the subject rotates about the Y axis. As we can see from the figure: 1) The pitch angles for upper spine, left shoulder and right shoulder are almost the same because the upper part of the back moves as a whole when the subject bends left and right. 2) the movement of the upper spine is much stronger than that of the lower spine, because the

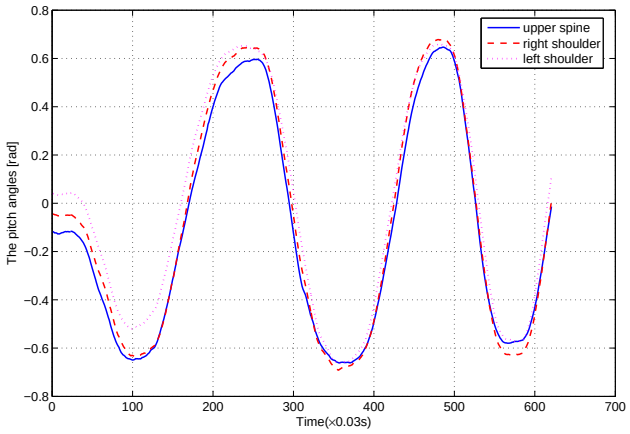

(a)

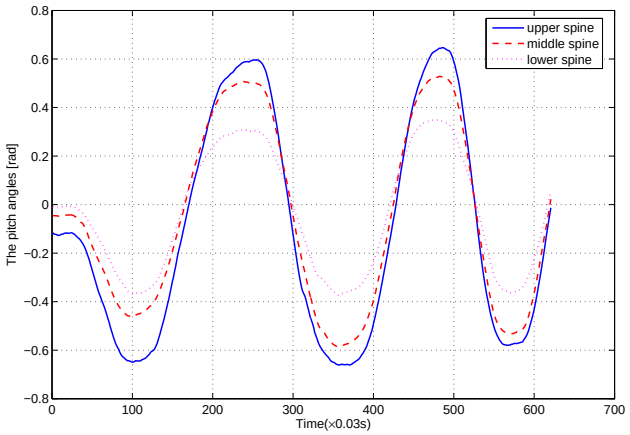

(b)

Figure 4. Pitch angles. (a) the pitch angle for upper spine, right shoulder and left shoulder; (b) the pitch angle for upper spine, middle spine and lower spine.

movement intensity and capability of the spine also decreases from the top spine to the bottom spine when bending left and right.

IV. Conclusion and Future Work

In this paper, we have presented a non-invasive and ubiquitous method to estimate the rotational human back movement in three dimensions using BSN sensor nodes, with each consisting of a three axis accelerometer, a gyroscope and a magnetometer. In our method, five BSN sensor nodes were used to put at the human back. Euler angles were then defined to represent the orientation for human back segments, kinematics analysis for the Euler angle was then derived, and an UKF was used to estimate the defined Euler angles. The experimental results have shown the feasibility and effectiveness of the proposed human back movement analysis method.

References

[1] T. Wong and R. Lee, "Effects of low back pain on the relationship between the movements of the lumbar spine and hip," *Human movement science*, vol. 23, no. 1, pp. 21–34, 2004.

[2] M. Cox, S. Asselin, S. Gracovetsky, M. Richards, N. Newman, V. Karakusevic, L. Zhong, and J. Fogel, "Relationship between functional evaluation measures and self-assessment in nonacute low back pain," *Spine*, vol. 25, no. 14, p. 1817, 2000.

[3] P. Reynolds, "Measurement of spinal mobility: acomparison of three methods," *Rheumatology*, vol. 14, no. 3, p. 180, 1975.

[4] M. Pearcy, J. Gill, M. Whittle, and G. Johnson, "Dynamic back movement measured using a three-dimensional television system," *Journal of biomechanics*, vol. 20, no. 10, pp. 943–949, 1987.

[5] M. Pearcy, "Stereo radiography of lumbar spine motion," *Acta Orthopaedica*, vol. 56, pp. 1–45, 1985.

[6] G. Yang, *Body sensor networks*. Springer-Verlag New York Inc, 2006.

[7] E. Foxlin, "Inertial head-tracker sensor fusion by a complimentary separate-bias kalman filter," in *Proceedings of the 1996 Virtual Reality Annual International Symposium*, 1996.

[8] H. J. Luinge and P. H. Veltink, "Measuring orientation of human body segments using miniature gyroscopes and accelerometers," *Medical and Biological Engineering and Computing*, vol. 43, no. 2, pp. 273–282, 2005.

[9] X. Yun and E. Bachmann, "Design, implementation, and experimental results of a quaternion-based Kalman filter for human body motion tracking," *IEEE Transactions on Robotics*, vol. 22, no. 6, pp. 1216–1227, 2006.

[10] D. Roetenberg, H. Luinge, and P. Slycke, "Xsens MVN: full 6Dof human motion tracking using miniature inertial sensors," 2009.

[11] R. King, D. Mcllwraith, B. Lo, J. Pansiot, A. McGregor, and G. Yang, "Body sensor networks for monitoring rowing technique," in *Wearable and Implantable Body Sensor Networks, 2009. BSN 2009. Sixth International Workshop on*, 2009, pp. 251–255.

[12] A. Chhikara, A. McGregor, L. Hadjilucas, F. Bello, and A. Rice, "Quantitative Assessment of the Motion of the Lumbar Spine and Pelvis with Wearable Inertial Sensors," in *2010 International Conference on Body Sensor Networks*, 2010, pp. 9–15.

[13] B. Lo and G. Yang, "Key technical challenges and current implementations of body sensor networks," in *Proc. 2nd International Workshop on Body Sensor Networks (BSN 2005)*, 2005.

[14] A. D. ADXL330, http://www.analog.com/en/sensors/inertial-sensors/adxl330/products/product.html.

[15] I. ITG-3200, http://invensense.com/mems/gyro/itg3200.html.

[16] H. HMC5843, www.magneticsensors.com/datasheets/HMC5843.pdf.

[17] P. Setoodeh, A. Khayatian, and E. Frajah, "Attitude estimation by separate-bias Kalman filter-based data fusion," *The Journal of Navigation*, vol. 57, no. 02, pp. 261–273, 2004.

[18] B. Ristic, S. Arulampalam, and N. Gordon, *Beyond the Kalman filter: Particle filters for tracking applications*. Artech House Publishers, 2004.

[19] Y. Bar-Shalom, X. Li, X. Li, and T. Kirubarajan, *Estimation with applications to tracking and navigation*. Wiley-Interscience, 2001.